Failure of Ti Plates for Oral and Maxillo-facial Surgery

A. P. Silva, G. Spera and C. Azevedo.
Instituto de Pesquisas Tecnológicas do Estado de São Paulo, Brazil

ABSTRACT*: The failure of titanium bone plates for oral and maxillo-facial surgery during use was investigated. Microstructural examination of a titanium plate revealed the presence of equiaxed a grains and intergranular platelets, which were identified as b phase. Fractographic examination revealed that fracture happened by a transgranular cleavage mechanism associated with secondary intergranular cracking (brittle fracture). Selective attack was observed to occur on the surfaces of the implant. These results indicated that the premature fracture of the miniplate was caused by hydrogen embrittlement.*

INTRODUCTION

Worldwide data reveals that 100 million metallic surgical implants were installed in human beings between 1940 and 1975 [1]. These implants are submitted to aggressive working conditions and their premature failure can be influenced by several factors, which include poor design; manufacturing mispractice and installation procedure [2-5]. In 1999, the Brazilian Government created the National Agency for Health Surveillance of Brazil (ANVISA) to promote the sanitary control of production and trade of medical and odontological products and services [5]. The agency is about to establish a general procedure to be adopted by health professionals and manufacturers in cases of failure of surgical implants [6,7]. The present paper deals with the metallurgical failure analysis of a titanium miniplate, which failed during use.

2- Results and Discussion

The experimental procedure consisted of visual inspection of the samples, macroscopic and microscopic characterisation of the material, fractographic investigation of the fracture surfaces and adjacent areas (electron scanning microscope equipped with energy dispersive spectrometer), X-ray diffractometry and analytical chemical analysis (plasma atomic emission spectrometer and inert gas fusion determinator). The chemical composition of

miniplate (see table 2) was in accordance with the requirements of ISO 5832-2, grade I. Commercially-pure (C.P.) titanium miniplates have been widely used in mandibular fracture fixation because of their strength and excellent biocompatibility [8]. Semi-quantitaive EDS microanalysis of the plate-screws indicated that they were manufactured in Ti-6Al-4V alloys (see table 2). Local manufactures advise the use of Ti-6Al 4V screws with Ti miniplates. The use of dissimilar metals in surgical implants, however, is not recommended [9] and further experiments will be carried out to investigate the galvanic corrosion. The miniplate failed along one of its recesses (see Figure 1a). The converging radial lines on the fracture surface and the presence of cracking on the lateral surface (see Figures 1b and 1c) indicated the origin of the fracture (miniplate lateral surface, , near the concave face). This surface was submitted during installation to tensile deformation (approximately 15° bending). The microstructure is formed by equiaxed α grains (ASTM grain size = 8) and intergranular platelets (see Figure 2a). The screws presented a microstructure composed of elongated α grains and intergranular β-platelets

TABLE 1 - Chemical composition (balance is titanium)

Material	%Al	%V	Fe	%O	%N	%C	%H
Ti miniplate	-	-	0.04	0.09	0.006	< 0.1	0.003
C.P. Ti grade 1	-	-	0.15 max.	0.18 max.	0.03 max.	0.1 max.	0.0125 max
Screws - mean	$4.6^{\pm}1.8$	$4.5^{\pm}0.4$	n.d.	n.d.	n.d.	n.d.	n.d.
Ti-6Al-4V alloy	5.5-6.75	3.5-4.5	-	0.2 max.	0.05 max.	0.08 max.	0.015 max

X-ray diffractometry (Cr Kα, 40.0 KV, step mode, $\Delta 2\theta$=0.0020º, t=40s) did not show the presence of TiH_2 or TiH phases, which may be responsible for the embrittlement of C.P. titanium [10-14]. The precipitation morphology suggests the presence of retained β-platelets instead [12-16]. The XRD results indicated the presence of 5 peaks of α phase - d= 2.555Å,$(100)_\alpha$; d= 2.3414Å, $(002)_\alpha$; 2.2431Å,$(101)_\alpha$, and 1.7269Å,$(102)_\alpha$ - and a possible peak of residual-β phase - d=1.6553Å,$(200)_\beta$. EDS microanalysis indicated that the platelets were richer in Fe (β-stabiliser element) than the matrix, see Figure 2c. Additionally, metallographic observation of Vickers hardness indentations (10 Kgf) showed the plastic deformation of platelets (see Figure 2b). These results suggested that

the intergranular precipitates are β-phase (not the brittle hydride phase) [17-20], which is typical in C.P. Ti due to the iron partitioning [21-22].

Fractographic investigation revealed the presence transgranular cleavage facets associated with secondary intergranular cracking (see Figure 3a). Detail of the fracture surface (see Figure 3b) showed intergranular cracking (arrow A); cleavage steps (arrow B) and "striation" marks (arrow C), indicating that the failure occurred by a brittle mechanism. High hydrogen content in the bulk metal (during dynamic load) or microvolumes (during sustained loading or fatigue cycling) may cause the embrittlement of Ti and Ti alloys [23]. The presence a fine discontinuous precipitation of β-phase may cause the embrittlement of near-α Ti alloys during dynamic [21] and sustained loading [22] as it acts as a hydrogen diffusion path. Microstructures containing thick continuous β platelets, however, are immune to embrittlement as β-phase tolerates hydrogen level close to its solubility limit without a significant loss in ductility [22, 23]. The presence of striation-like markings (see Figures 4a and 4b) were previously associated with cracking-arrest markings produced by discontinuous crack propagation (repeated formation and rupture of the brittle stress-induced hydride phase) [17-19]. William [24] explained that these markings are the intersections of intense slip bands with the fracture surface.

Figures 4a and 4b show the aspect of lateral and convex surfaces of the miniplate, indicating the occurrence of preferential attack and resembling microbiologically influenced corrosion, which may have acted as hydrogen source [25]. Finally, Koch [20] stated that the fracture produced by stress corrosion cracking (SCC) and slow-strain rate hydrogen embrittlement are indistinguishable in near-α alloys. They consist of cleavage-like facets within each α-plate, each facet presenting surface steps and parallel secondary cracking. The fracture occurs occur through the α-phase due to the formation of brittle stress- hydride phase. High quality pure titanium implants should present a special anodised surface finish that increases the thickness of the protective oxide film and, therefore, the corrosion resistance [26]

REFERENCES

1- Smith,G.K. and Black.J. (1976) In: Symposium on retrieval and analysis of orthopedic implants, NBS Special Publication 472, 23-30.

2- Pohler, O.E.M. (1986) In: Metals Handbook. ASM International. 9th Ed. **v.11**, 668-694.
3- Dumblenton, J.H. & Miller, E.H. (1975) In: Metals Handbook. ASM International. 8th Ed. **v.10**, 571-580.
4- Piotrowski,G. (1976) In: Symposium on Retrieval and Analysis of Orthopedic Implants. NBS Special Publication 472, 41-49.
5- Azevedo, C.R.F and HippertJr., E. (2001) Pract. Failure Analysis, **11**, 53-61.
6- FDA (1996) Medical device reporting: an overview. Center for Devices and Radiological Health, Food and Drugs Administration, 14 p.
7- Medical Devices Agency (1998) European Commission Guidelines <www.medical-devices.gov.uk/mda-aic.htm#report>.
8- Torgensen, S.E. and Gjerdet, N.R. (1995) Retrieval study of stainless steel and Ti miniplates used in maxillofacial surgery. <www.uib.no/cris/dok2>.
9- R.W. Shutz and D.E. Thomaz (1987) In: Metals Handbook. ASM International, 9th Ed., **vol. 13**, 669- 706.
10- Kessler, H.D., Sherman, R.G. and Sullivan, J.F. (1955) J. Metals, **7**, 242-252.
11- Williams, D.N. (1962) Journal of the Institute of Metals, **91**, 147-152.
12- Nishigaki, M., Tanabe, A., Ito, Y. and Moriguchi Y. (1980) In: Proc. Intern. Conf. on Titanium, AIME, 1663-70.
13- Carter, T.J. and Cornish, L.A. (2001) Eng. Failure Analysis, **8**,113-21.
14- Ito, H.L. (1982) MEng Thesis, Escola Politécnica da Universidade S. Paulo.
15- Paton, N.E., Hickman,B.S. and Lesli,D.H. (1971) Metal. Trans., **2**, 2791- 96.
16- Hall, I.W. (1978) Metal. Transactions, **9A**, 815-20.
17- Nelson, H.G. (1976) Metal. Transactions **7A**, 621-27.
18- Meyn, D.A. (1972) Metal. Transactions, **3**, 2302-5.
19- Nelson, H.G, Williams,DP and Stein,E.S. (1972) Metal. Trans., **3**, 469-75.
20- Koch,G.H., Burle,A.J., Liu,R. and Pugh,E.N. (1981) Metal. Trans. **12A**, 1833-43.
21- Puttlitz, K.J. and Smith, A.J. (1980) in: Proc. Intern. Conf. on Titanium, AIME, 427-34.
22- Hack, J.E. and Leverant, G.R. (1982) Metal. Trans. ,13A,1729-38.
23- Kolachev, B.A., Vigdorchick, S.A., and Malkov, A.V. (1980) In: Proc. Intern. Conf. on Titanium, 1663-70.
24- William, J.C., Sommer, A.W., Tung, P.P. (1972) Metal. Trans. **3**, p.2979
25- Biezma, M.V. (2001), International Journal of Hydrogen Energy, **26**, 515-20.
26- Disegi, J.A. (1994) In: AO/ASIF Instruments and Implants. R. Texhammar and C. Colton, Springer Verlag, 2nd Edition.

(a)

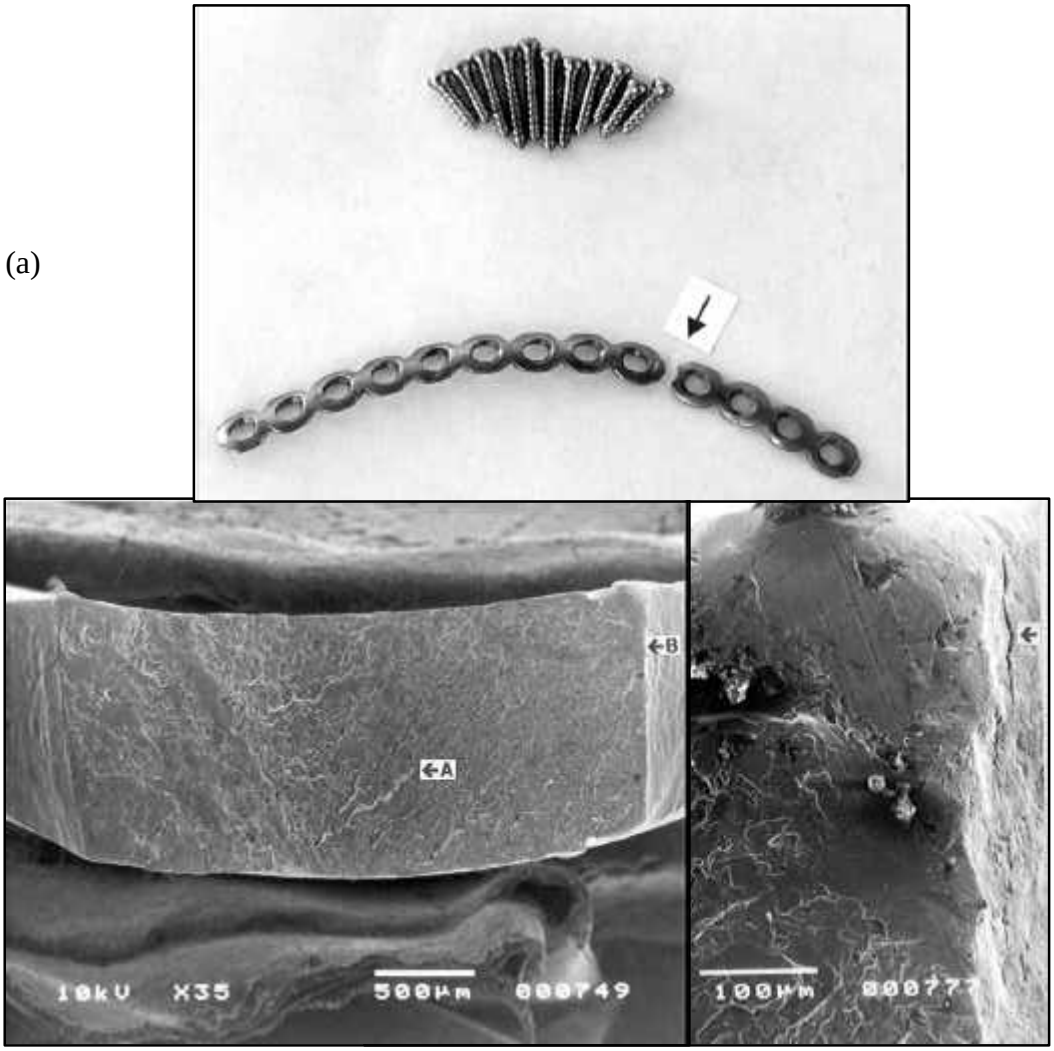

(b) (c)

Figure 1 : a) Failed oral maxillo-facial plate for jaw reconstruction (see arrow); b) General view of the fracture surface showing radial lines (see arrow A) converging to the fracture origin (see arrow B)[1]; c) Detail of the fracture origin, lateral plate surface, revealing the presence of cracking (see arrow).

[1] Miniplate concave face lies in contact with the bone.

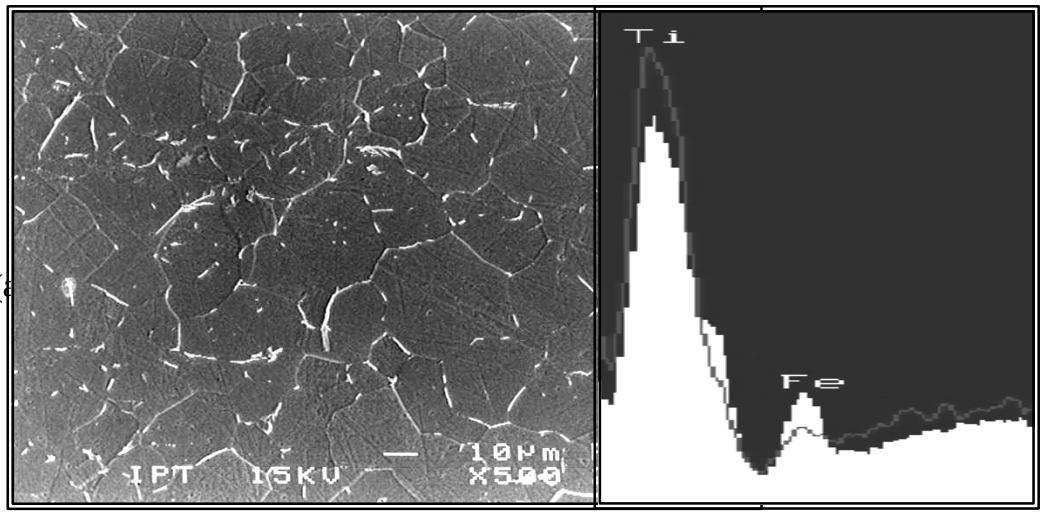

(a) (b)

(c)

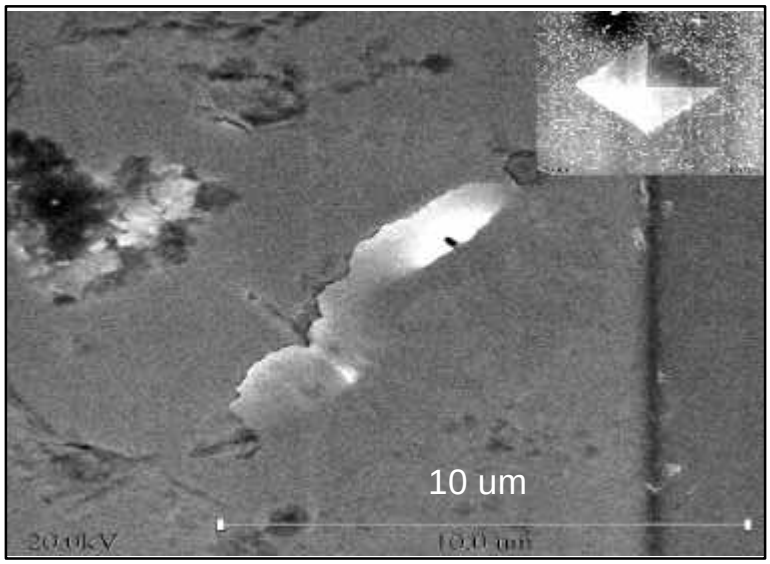

Figure 2 : a) Detail of the microstructure showing equiaxed α grains and intergranular platelets; b) EDS analysis showing matrix (line spectra) and Fe-rich precipitate (solid spectra), Ti-Lα and Fe-Lα peaks; c) Detail of the precipitate deformation inside the Vickers indentation zone (see top-right).

(a)

(b)

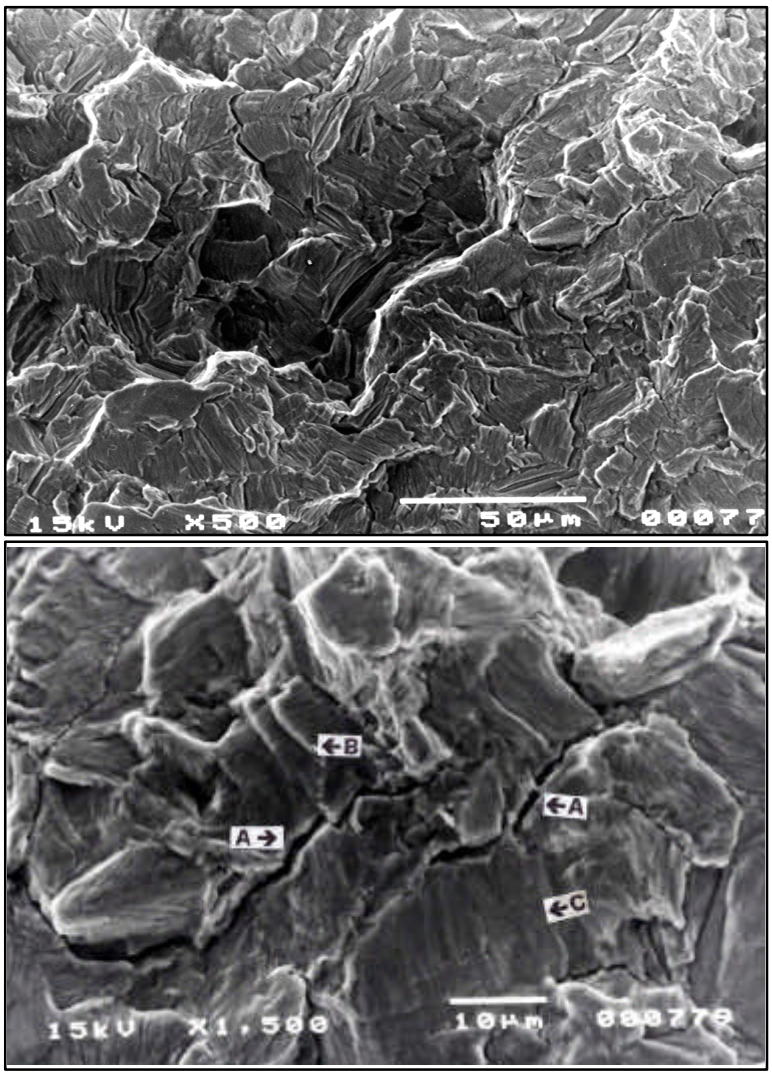

Figure 3 : a) Detail of the fracture surface near the fracture origin revealing transgranular cleavage associated to secondary intergranular cracking (brittle fracture); b) detail of the brittle fracture surface showing intergranular cracking (arrow A); cleavage steps (arrow B) and slip traces (arrow C).

(a)

(b)

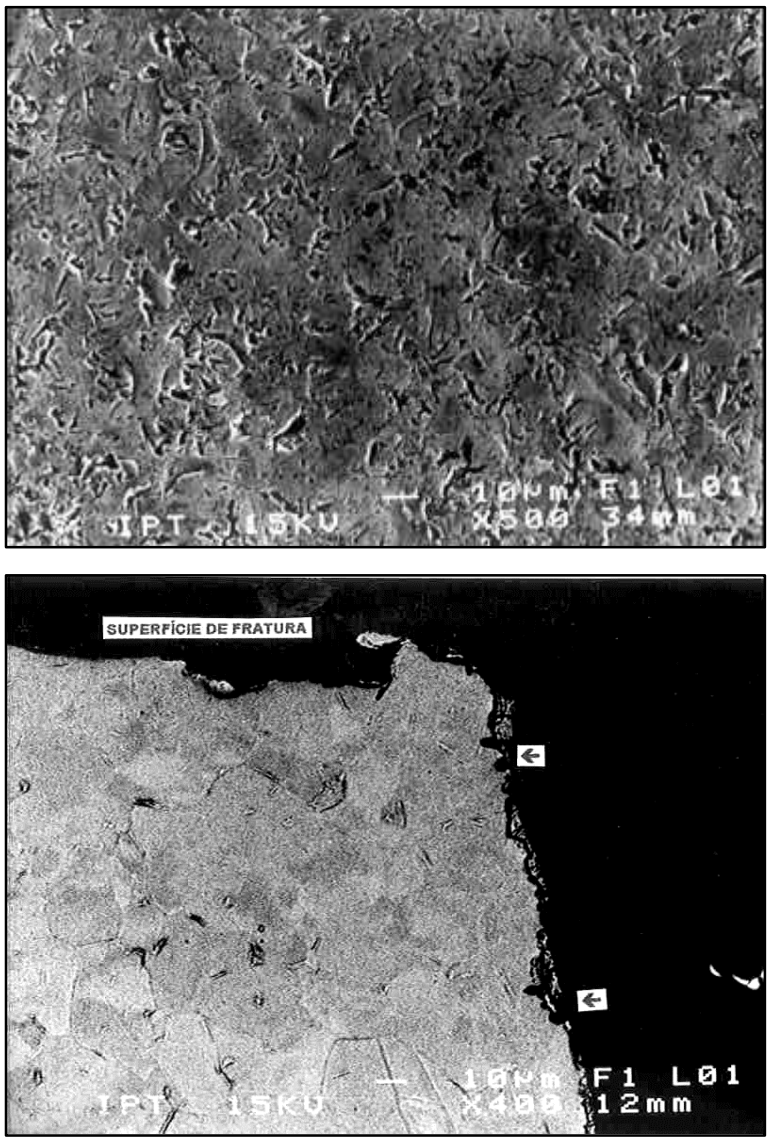

Figure 4 : Detail of the miniplate convex face: a) top view showing localised etching found on the miniplate convex face and lateral surfaces; b) longitudinal cross section showing the depth of the hydriding layer and the presence of localised etching on the convex surface (see arrows).